

1 **Development trajectory of an integrated framework for the mitigation**
2 **of future flood risk: results from the FloodLand project**

3 Ismaïl Saadi^a, Martin Bruwier^b, Ahmed Mustafa^a, Yann Peltier^b, Pierre
4 Archambeau^b, Sébastien Erpicum^b, Philippe Urban^c, Alain Dassargues^c,
5 Benjamin Dewals^b, Michel Piroton^b, Jacques Teller^a, Mario Cools^{a,d,e}

6 *^aUniversity of Liège, ArGEnCo, Local Environment Management & Analysis (LEMA),*
7 *Liège, Belgium*

8 *^bUniversity of Liège, ArGEnCo, Hydraulics in Environmental and Civil Engineering*
9 *(HECE), Liège, Belgium*

10 *^cUniversity of Liège, ArGEnCo, Hydrogeology and Environment Geology, Liège,*
11 *Belgium*

12 *^dKULeuven Campus Brussels, Department of Informatics, Simulation and Modeling,*
13 *Brussels, Belgium*

14 *^eHasselt University, Faculty of Business Economics, Diepenbeek, Belgium*

15

16 Corresponding author: Mario Cools, University of Liège, ArGEnCo, Local
17 Environment Management & Analysis (LEMA), Quartier Polytech 1, Allée de la
18 Découverte 9, BE-4000 Liège, Belgium, Email: mario.cools@ulg.ac.be

19

20 **Development trajectory of an integrated framework for the mitigation** 21 **of future flood risk: results from the FloodLand project**

22 In this paper, the development trajectory of an integrated framework for the
23 mitigation of future flood risk of the Ourthe river basin in Belgium is discussed.
24 The paper contributes to the state-of-the-art by presenting an integrated
25 multidisciplinary framework capable of making long-term projections (time
26 horizon 2050 and 2100) with the objective of mitigating future flood risk by
27 proposing alternative land-use scenarios. It bridges numerous different fields,
28 including urban planning, transport engineering, hydrology, geology,
29 environmental engineering and economics. The overall design and validation
30 results of the different sub-modules of the framework are presented, and ongoing
31 and future enhancements are highlighted.

32 Keywords: river floods, development trajectory, land-use transport interaction
33 model, hydrologic model, hydraulic model

34 **1. Introduction**

35 Worldwide, floods are the most frequent natural disasters and cause over one-third of
36 overall economic losses due to natural hazards (Munich RE; He et al. 2011). For many
37 river basins, studies show that the flood risk will further increase during the 21st century
38 as a result of climate change. However, climatological changes will not be the only
39 increasing factor of future flood risk. Societal changes, induced by economic
40 development and exhibited by changes in land-use, can affect future flood risk through
41 multiple pathways, including climate (e.g., modified evapotranspiration), run-off in the
42 catchment (reduced infiltration), inundation flows (obstruction by buildings) and flood
43 exposure (higher value of elements-at-risk in the floodplains).

44 Compared to the vast body of literature regarding the influence of climate
45 change on hydrological extremes, less research has addressed the influence of land-use
46 changes on flood risk (Beckers et al. 2013; Thielen et al. 2014). Among the few

47 existing studies, some suggest that land-use change, in the form of urban sprawl, could
48 be the overwhelming contribution to future rises in flood risk (Poelmans, Van
49 Rompaey, and Batelaan 2010; Elmer et al. 2012). Nonetheless, the impact of land-use
50 change on flood exposure and vulnerability has not yet been studied at a sufficiently
51 fine spatial scale to capture the relevant process governing future flood risk in urbanized
52 floodplains.

53 Thus far, no study has combined future land-use modeling with building-scale
54 inundation modeling, exposure analysis and damage assessment. This is especially true
55 when interactions between land-use and transportation are also explicitly taken into
56 account. The latter interactions are important, as disruptions in the transportation
57 infrastructure cause severe strains on society. Failures and disruptions in the
58 transportation system negatively affect activity-travel patterns and business operations
59 (Jenelius and Mattsson 2015; Sohn 2006; Suarez et al. 2005).

60 This paper contributes to the state-of-the-art by presenting the development
61 trajectory of an integrated multidisciplinary framework that is capable of making long-
62 term projections (time horizon 2030 and 2100) with the objective of mitigating future
63 flood risk by proposing alternative land-use scenarios. It bridges numerous different
64 fields, including urban planning, transport engineering, hydrology, geology,
65 environmental engineering and economics. The study area for this development is the
66 river basin of the Ourthe in Belgium (displayed in Figure 1). However, note that, for the
67 development of different submodules of the framework, a larger geographical scope is
68 envisaged. This is particularly the case for sub-models that assess effects surpassing the
69 boundaries of the study area, such as the estimation of reduced business activities in the
70 occurrence of river floods.

71



72
73 Figure 1. Map of the study area.

74
75

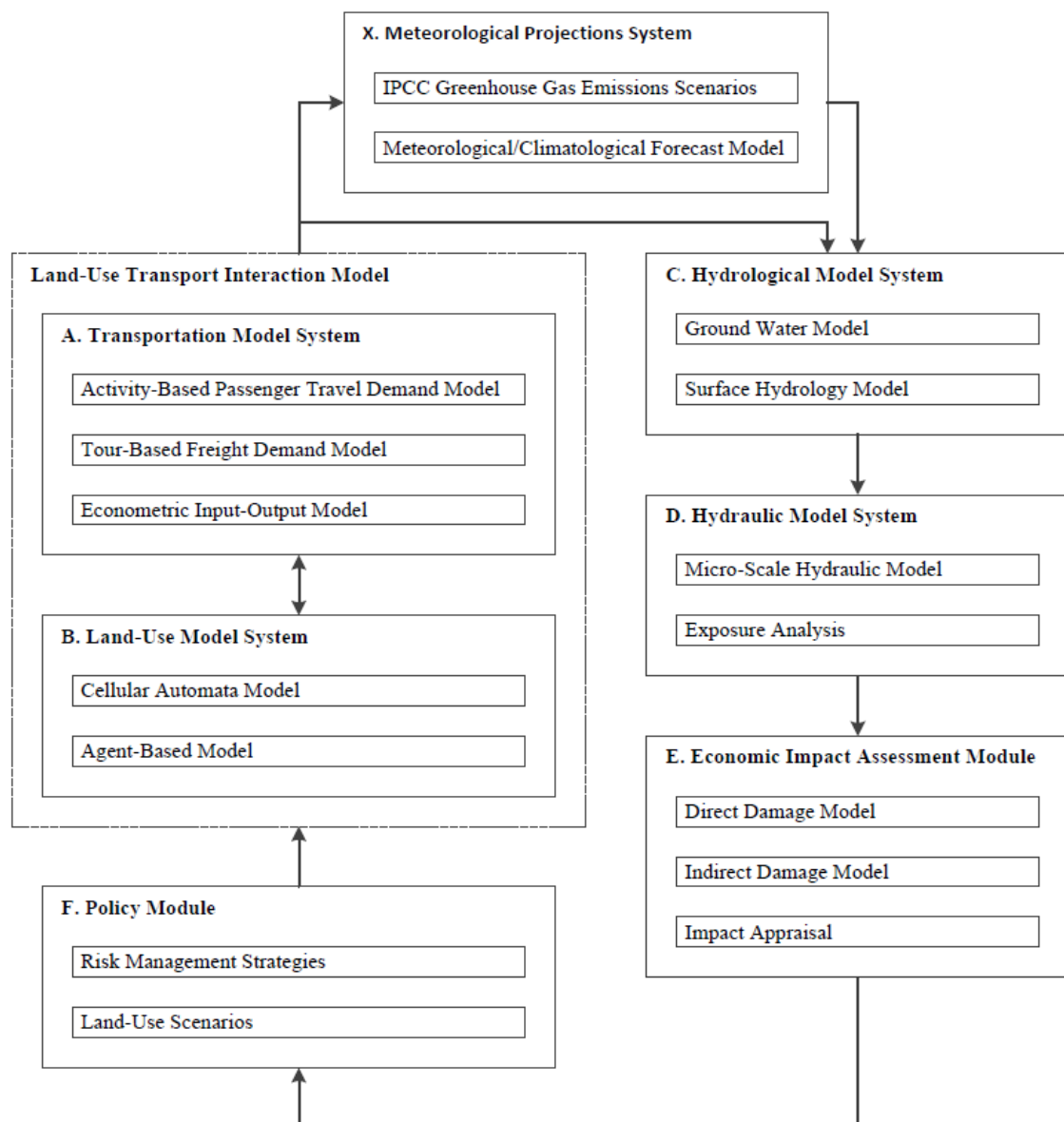
76 The remainder of the paper is organized as follows. In Section 2, an overview of
77 this framework is provided, and the already developed sub-models and their validation
78 results are presented. Further enhancements and future developments are discussed in
79 Section 3, and finally, a wrap-up of the most important findings is provided in Section
80 4.

81

82 2. Integrated framework

83 2.1. Design

84 An overview of the integrated framework is displayed in Figure 2. The framework
 85 consists of five primary modules that are strongly connected. Note that the arrows in
 86 this scheme represent the most important flows of the modeling process.



87

88 Figure 2. Integrated flood-risk mitigation framework.

89 The starting point for the long-term forecasts is the meteorological projection

90 system [X], which uses the greenhouse gas emission scenarios defined by the
91 intergovernmental panel on climate change (IPCC) as an exogenous input to direct the
92 climatological forecasts in terms of future precipitation levels and temperatures. The
93 potential of using the climate scenarios provided by IPCC in the context of the
94 quantification of hydrological impacts of climate change has been underlined in the
95 literature (Drogue et al. 2004; Kundzewicz et al. 2005; van Pelt et al. 2009;
96 Vansteenkiste et al. 2013; Jun et al. 2013). The climatological/meteorological forecasts
97 are obtained by global circulation models (GCM) and regional climate models (RCM).

98 The forecasts concerning future precipitation levels and temperatures are used as
99 an input for the hydrological model system [C]. The water transfers at the catchment
100 level are modeled with a physically based and spatially distributed model, which
101 couples surface and groundwater flows. The main results of these simulations are series
102 of calculated river discharges at different locations in the watershed. They are further
103 used to establish flood-frequency curves.

104 These flood-frequency curves are then used as an input to the hydraulic model
105 system [D] that estimates the inundation extent and depth, and this enables an exposure
106 analysis to estimate the elements at risk.

107 Once the elements at risk are determined, the cascade of economic damages is
108 valued by separating the direct economic damage (e.g., economic damage related to
109 business interruption) and the cascade of indirect effects (e.g., loss of connectivity
110 within the broader economic region) in the economic impact assessment module [E]. To
111 this end, input-output models provide an adequate methodology to capture the workings
112 of an economic system and the influence of disturbances therein (Jonkman et al. 2008).
113 An overview of input-output models, which make the direct linkage with land-use
114 transport interaction models, is provided by Bachmann, Kennedy, and Roorda (2014).

115 The appraisal of the total economic impact will then allow for the development
116 of policy scenarios [F] that can mitigate this impact. Policy scenarios can be separated
117 in specific spatial planning scenarios, as can policy measures that focus on policy
118 engagement in the context of water resource management. The effect of the land-use
119 scenarios will then be evaluated by the land-use transport interaction model, which
120 consists of a land-use model system [B] and a transportation model system [A]. In turn,
121 the altered land-use and transport patterns will be used as an input to the hydrological
122 model system, as well as for the meteorological projections.

123 ***2.2. Sub-model development***

124 *2.2.1. Land-Use Transport Interaction Model*

125 A key element in the development of the mitigation forecasting framework is the land-
126 use transport interaction (LUTI) model, as it provides the forecasts for changes in land-
127 use and transport infrastructure. The explicit choice to opt for the development of an
128 LUTI model is motivated by the crucial aspect of transport infrastructure in future land-
129 use development, e.g., the significance of proximity to road infrastructure in future
130 constructions (Mustafa et al. 2015a), and the impact of land-use in terms of activity
131 opportunities on the transport pattern. In the current state of development of the LUTI
132 model, the "transport → land-use" feedback is already fully incorporated, whereas the
133 "land-use → transport" feedback is not yet fully incorporated.

134

135 *2.2.1.1. Transportation Model System.* The implementations with regard to the
136 development of the transport model system can be broadly categorized into (i) the
137 development of a travel demand model for freight transport, which will become

138 integrated with the input-output model, and (ii) the development of an activity-based
139 travel demand model.

140 The development of the travel demand model for freight transport is especially
141 important in the context of the chain of higher-order effects when different production
142 facilities are affected. Current developments have thus far focused primarily on the
143 development of a four-step model, as it is reasonably adopted for goods transport
144 modeling (Holguín-Veras et al. 2014). With respect to the first step, i.e., trip generation,
145 the challenge mainly lies within the collection of sufficiently detailed data to make sure
146 that perhaps the most import step of the four-step model is calibrated with acceptable
147 precision. In this regard, recommendations, formulated in the 2012 dedicated NCFRP
148 report (Lawson et al. 2012), were taken into account. To perform the model estimation,
149 data stemming from a detailed survey of retail activities (Devillet, Jaspard, and Vazquez
150 Parras 2014) were used. In particular, location information and industrial sector
151 information (NACE code), as well as the value of assets in the trade sector, were used
152 as inputs. Moreover, statistics provided by the Belgian federal ministry for economy
153 were adopted to increase the model accuracy. Regarding the second step, i.e., trip
154 distribution, we opted for a gravity model, as the properties facilitate integration with an
155 input-output analysis. Concerning modal choice, the current model focuses mainly on
156 truck transport, which is further assigned to the road network in the fourth step using a
157 deterministic user-optimal equilibrium assignment.

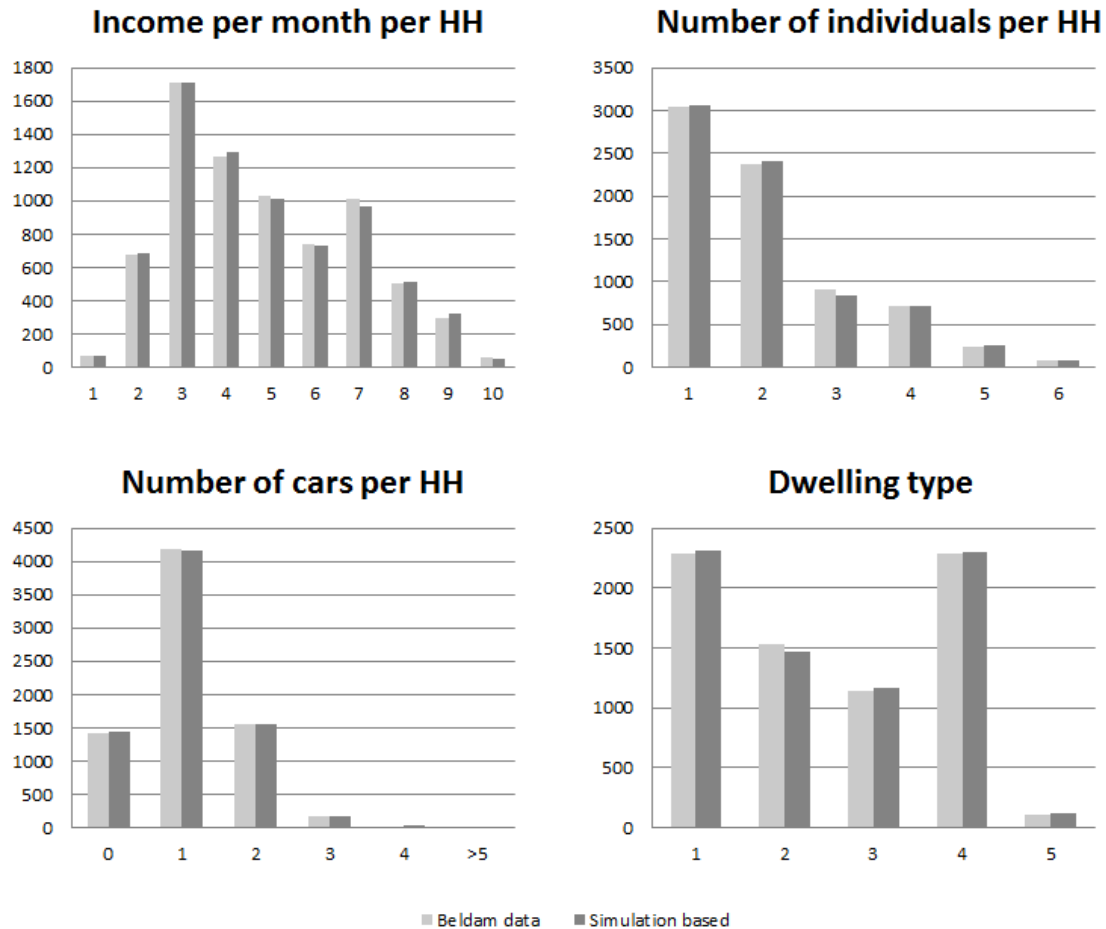
158 With respect to the development of the activity-based travel demand model,
159 research efforts have focused on the development of a large-scale agent-based micro-
160 simulation model. The purpose of this agent-based micro-simulation approach is the
161 prediction of travel patterns of a given population on the transportation network. The
162 disaggregated nature of agent-based micro-simulation models allows for higher

163 temporal and spatial resolutions compared to more conventional models (Rasouli and
164 Timmermans 2014; Henson et al. 2009).

165 Running agent-based models requires a base year population. In this context, a
166 synthetic population is generated as a key input. Afterward, agents are assigned activity
167 chains through an activity-based generation process. Finally, the synthetic population,
168 along with the network, is integrated into a dynamic traffic assignment simulator.

169 Concerning the generation of synthetic populations, many methodologies have
170 been developed during the last few decades, such as Iterative Proportional Fitting (IPF)
171 (Beckman, Baggerly, and McKay 1996; Guo and Bhat 2007; Pritchard and Miller 2012)
172 and Iterative Proportional Updating (IPU) (Ye et al. 2009; Pendyala et al. 2012). More
173 recently, an original technique based on a Markov Chain Monte Carlo (MCMC)
174 algorithm (Gibbs sampler) was presented as an alternative to the standard approaches
175 (Farooq et al. 2013). According to Farooq et al.'s results, the MCMC method clearly
176 outperforms the previous ones. Therefore, this methodology has been preferred here for
177 its higher accuracy. To perform the population synthesis, data from the Belgian national
178 household travel survey (BELDAM) (Cornelis et al. 2012) were used. As a first attempt,
179 the most relevant variables related to households (income, household size, number of
180 cars, and dwelling type) were extracted. When applying the simulation-based technique,
181 results show a strong match between real and predicted population attributes, as
182 illustrated by Figure 3 and documented in Saadi et al. (2016d).

183



184

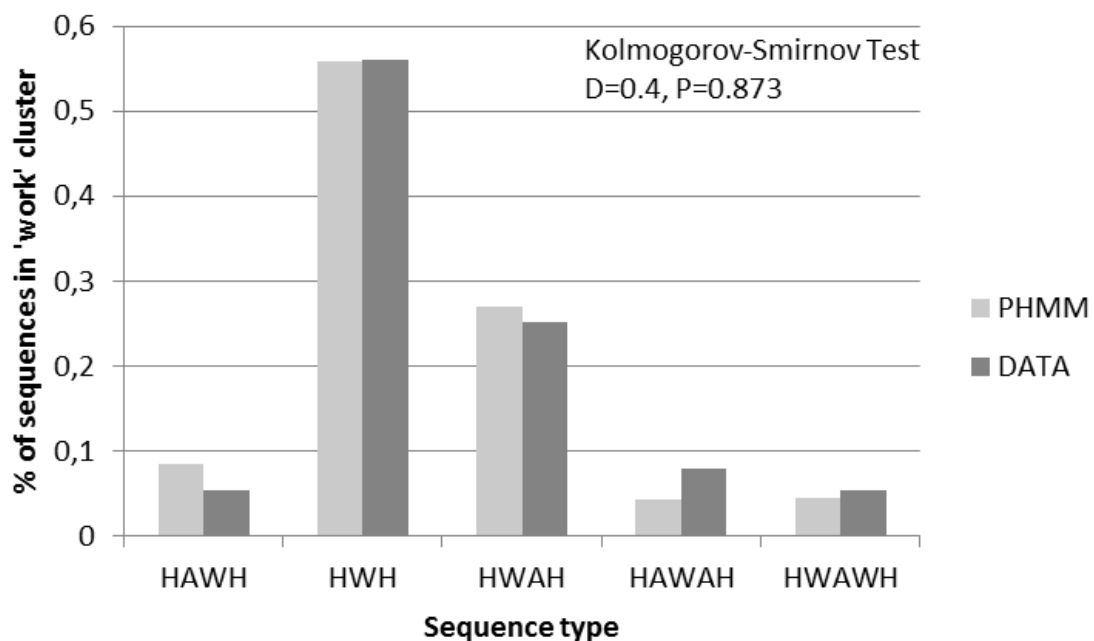
185 Figure 3. Comparison between the simulation-based population synthesis approach and
 186 BELDAM.

187

188 Regarding the prediction of activity-travel patterns, several improvements have
 189 been realized during the last few decades, but these prediction models still need to be
 190 further enhanced (Rasouli and Timmermans 2014; Auld and Mohammadian 2009). In
 191 this context, we opted for the approach suggested by Liu et al. (2015) using the profile
 192 Hidden Markov Model (pHMM). This technique learns the structure of pre-established
 193 activity chains extracted from activity-travel diaries. Consequently, agent activity chains
 194 can be randomly generated from the pHMM model. This technique is particularly
 195 flexible since it characterizes both short and long activity chains. Moreover, it is capable
 196 of identifying regular and irregular activities within each cluster, as well as their

197 sequential order. In accordance with the population synthesis, data from the Belgian
 198 national household travel survey were used to calibrate the model. Originally,
 199 BELDAM data are organized according to trips. Thus, a transformation of the dataset
 200 into activity chains was necessary before running the model. Moreover, simulations are
 201 focused on generating only activity chains related to the “work” cluster. Individuals
 202 whose longest activity is work belong, by definition, to this specific cluster. The results
 203 obtained thus far are very promising (Saadi et al. 2016a, 2016b). The agreement
 204 between predicted and observed activity chains is relatively high. According to the
 205 Kolmogorov-Smirnov statistical test, the two distributions reveal a p-value of 0.87
 206 (Figure 4).

207



208

209 Figure 4. Comparison between the predicted activity sequences and BELDAM.

210

211 Finally, the generated activity-travel sequences are then assigned to the network
 212 using a dynamic traffic assignment (DTA) simulator. To this end, the DTA module
 213 developed within the context of MATSIM (Balmer, Axhausen, and Nagel 2006) was

214 used. Details of the integration procedure can be found in Saadi, Teller, and Cools
215 (2016).

216 2.2.1.2. *Land-Use Model System.* To understand ongoing and future urban
217 dynamics, a comprehensive analysis of land-use changes is required. This
218 understanding is also a key factor in evaluating the flood risk at different spatial scales.
219 Recall from Figure 2 that the effects of spatial planning scenarios to mitigate the
220 negative effects of river floods are calculated using the land-use model-system and that
221 the outputs are then coupled with the hydrological models, as suggested by Poelmans,
222 Van Rompaey, and Batelaan (2010). The most common methods for modeling land-use
223 change are Cellular Automata (CA) (Aljoufie et al. 2013; Batty, Xie, and Sun 1999;
224 García et al. 2011; Guan et al. 2011; Mitsova, Shuster, and Wang 2011) and Agent-
225 Based (AB) methods (Augustijn-Beckers, Flacke and Retsios 2011; Bert et al. 2011;
226 Hosseinali, Alesheikh, and Nourian 2013; Ralha et al. 2013). Other artificial
227 intelligence approaches have also been used to forecast land-use change (Du et al.
228 2010).

229 Generally speaking, CAs are based on spatial inferences considering a series of
230 territorial variables (distance to roads, distance to cities, slope, etc.), as well as
231 neighborhood effects. ABs simulate the behavior of agents, such as households,
232 companies, etc. For the simulations until 2030, a CA-based approach has been
233 developed, whereas for the 2100 simulations, an integrated framework is developed
234 combining the strengths of the CA- and AB-based approaches.

235 A CA model using Corine Land Cover (CLC) data has been developed. It
236 focuses on urban cells (residential, industrial, commercial, etc.). The model considers
237 built-up change probabilities based on three sets of transition rules: neighborhood
238 effects, a suitability map and a stochastic component.

239 Based on explanatory variables, such as the distances to main roads and cities, a
240 suitability map has been developed using a binomial logistic regression model. Its
241 quality has been assessed (validated) using a Relative Operating Characteristic (ROC)
242 procedure. The ROC value ranges from 0.5 for a model that assigns the probability
243 randomly to 1 for a model that perfectly assigns the probability of change. The ROC of
244 our suitability map is 0.742 (Mustafa et al. 2014). In comparison, ROC values for a
245 number of suitability maps reported in other studies range from 0.62 to 0.74 (Pontius,
246 Huffaker, and Denman 2004).

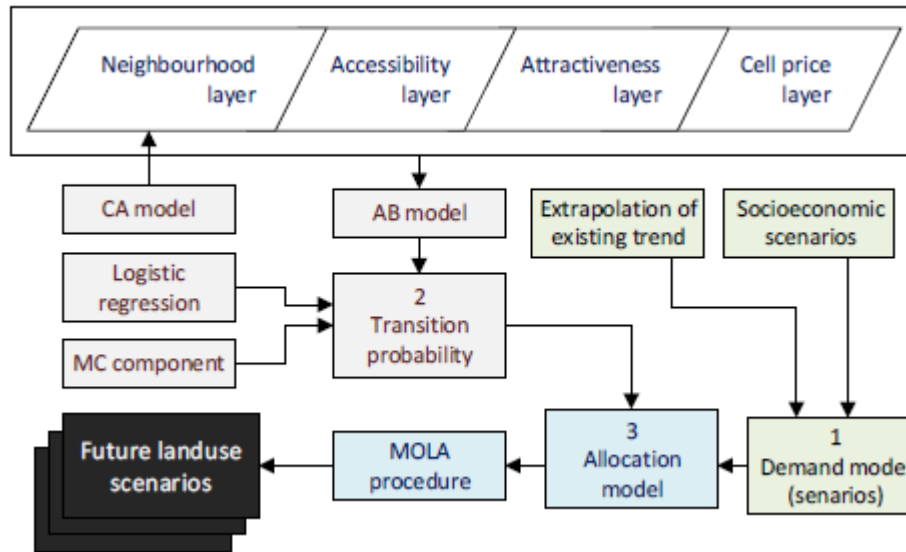
247 Regarding the development of the CA model, the following challenges have
248 been identified. First, we were confronted with limitations inherent to the datasets used.
249 Three datasets are utilized for land-use data: COSW, Corine Land Cover (CLC) and
250 CADastral data (CAD). COSW is provided with a very short time span (2001, 2003 and
251 2005), which means it is not applicable for long-term forecast modeling. CLC covers a
252 longer time span (1990, 2000 and 2006), but it still remains far too short for modeling
253 the 2100 horizon. Moreover, the standards of CLC have changed over time, affecting
254 the comparability of data. CAD data can be used for longer time frames as it provides
255 the date of construction of each building, but only built-up land-use types can be
256 derived from this dataset (Mustafa et al. 2015b). Secondly, with respect to the spatial
257 resolution, it is important to analyze the model outcomes at different resolutions to
258 determine whether the model is sufficiently detailed at a specific resolution. Our model
259 has been validated for several resolutions up to 6,400 m \times 6,400 m. The results
260 show that the model begins to perform well for a resolution above approximately 800 m
261 \times 800 m, which is not yet sufficient for coupling with inundation models.
262 Finally, land-use models are subject to uncertainties due to local unpredicted factors,
263 such as real estate retention and administrative decisions. A stochastic perturbation

264 component has been introduced in the CA model to handle these local uncertainties
265 (Pontius, Huffaker, and Denman 2004). The model was calibrated using different
266 magnitudes of randomness to determine whether the stochastic perturbation component
267 is sufficient to handle these effects. The results show that our model accuracy increased
268 as a result of the introduction of a stochastic perturbation component with a very small
269 magnitude of randomness. Nonetheless, such a stochastic perturbation fails to address
270 some spatial properties of observed land-use changes, especially the evolution of the
271 size and the number of urbanized patches observed in the past.

272 The validation of different model runs has been evaluated by calculating the
273 cell-to-cell agreement and by measuring the spatial properties. The cell-to-cell
274 agreement of our model due to location is approximately 91.9% for all built-up cells and
275 approximately 29% for newly built-up cells, which lies well within the value ranges
276 reported in the literature (Wang et al. 2013).

277 To ensure that the framework is sensitive to conditions that have never been
278 observed in the past, the final model integrates AB and CA sub-models. Using this
279 integration, the model will not only simulate the extrapolation of observed changes, it
280 will also consider the preferences of households. In addition, the model couples
281 deterministic process-based components with a stochastic component to better handle
282 uncertainty due to global unpredicted factors, such as population growth and population
283 movements. An overview of the integrated model is presented in Figure 5. The model
284 includes the following three main components: a demand model, the calculation of the
285 transition probabilities and an allocation model.

286



287

288 Figure 5. Integrated CA-AB land-use change modeling framework.

289

290 The demand model calculates the quantity of change of urban lands. Different
 291 scenarios of the quantity of change will be estimated by the following two methods: (i)
 292 a simple linear extrapolation of the past change trends and (ii) the use of socioeconomic
 293 factors to estimate future growth.

294 The transition probability of each undeveloped cell (non-urban) will be
 295 calculated using different components. The AB model calculates the transition
 296 probability using the following four layers (maps): neighborhood weights, accessibility,
 297 attractiveness and expected cell price. An agent represents a cell developer, and each
 298 undeveloped cell will be linked to an agent. Each agent will seek an appropriate cell to
 299 develop based on maximizing his profits. Each agent will develop one cell per time step
 300 (one year). Utility functions will be used to assign scores for each undeveloped cell
 301 based on the mentioned four layers. The neighborhood weights layer will be developed
 302 using the CA model. Other factors and parameters will be set using existing data, expert
 303 knowledge and data sensitivity analysis for various values of the parameters of each
 304 group. The AB model starts by selecting one agent randomly and then calculates a score

305 for each undeveloped cell based on the agent category. The agent selects the cell with
306 the best score. The model verifies whether the selected cell was already selected by
307 another agent in a previous iteration. If this is the case, the model determines the winner
308 (the richest one). A more elaborate description of the AB model is provided in Mustafa
309 et al. (2015b).

310 Finally, the allocation model uses a Multi-Objective Land Allocation (MOLA)
311 procedure to allocate the required quantity of growth. MOLA ranks cells according to
312 their transition probability and selects cells with the highest relative ranking until it
313 meets the requested quantity.

314 2.2.2. Meteorological Projections System

315 The assessment of the discharge statistics for the risk analysis requires continuous
316 simulations with a physically based hydrological model using data time series of rainfall
317 and temperature as input. To investigate future time horizons, the existing time series of
318 meteorological observations (precipitation and temperature) need to be disturbed
319 according to different climate change scenarios. The selection of an appropriate method
320 to compute and apply the necessary disturbances is a twofold challenge, as the
321 perturbed series must be representative of the future climate of Belgium and the overall
322 consistency of the entire modeling procedure must be ensured (e.g., the time resolution).

323 Two methods of perturbation were compared in terms of suitability for long-
324 term projections: (i) the CCI-HYDR tool from KU Leuven and (ii) the Advanced Delta
325 Change method from the KNMI. A third approach was also considered, coupling a
326 perturbation method and a stochastic weather generator. Although this method seems
327 the most appropriate from a theoretical perspective, the use of a stochastic weather
328 generator would introduce additional sources of uncertainty in the risk analysis and
329 further increase the computational burden for the subsequent hydrological modeling. All

330 three methods have been previously used in research dealing with hydrological impacts
331 of climate change (Bruwier et al. 2015) and were validated in dedicated studies
332 (Goderniaux et al. 2011; van Pelt et al. 2012; Ntegeka et al. 2014; Goderniaux et al.,
333 2015).

334 The two retained approaches are based on a modified delta change method for
335 estimating the perturbation factor from the comparison between meteorological
336 variables during the control period of 1961-1990 and the results from various GCM and
337 RCM at different future horizons. This perturbation factor is then used to perturb the
338 observed rainfall and temperature time series. The resulting perturbed time series are 30
339 years long and stationary and they are representative of the climate at the designated
340 target year or period.

341 More specifically, the CCI-HYDR tool proposes only three distinct scenarios
342 (wet, mean, dry), which differ mainly in the results for rainfall (and not for
343 temperature). Using this method enables the number of runs of the hydrological model
344 to be reduced; however, uncertainties in the risk evaluation may remain, as in the end,
345 only a limited number of estimates of future flood discharges are available. In contrast,
346 the KNMI-ADC method includes 191 scenarios, which enables a broad range of
347 possible climate changes to be explored. Nonetheless, using this complete set of
348 scenarios in combination with a physically based hydrological model would simply not
349 be computationally tractable. As a consequence, prior choices have to be made within
350 the set of scenarios, which is, in essence, the principle followed by the CCI-HYDR
351 approach.

352 Based on the conducted comparison, the CCI-HYDR method was considered as
353 the most suitable, as it overcomes serious disadvantages of the other methods with
354 respect to the choice of scenarios, time-resolution and applicability. Nonetheless, in its

355 standard form, this method perturbs separately the time series of different gauges of the
356 same catchment. This would lead to an artificial loss of the existing correlations
357 between gauges located in the same area. Therefore, the CCI-HYDR tool has been
358 adapted to perform perturbations of the time series at several gauges simultaneously,
359 such that the correlations between these stations are preserved. This adapted version of
360 the CCI-HYDR tool was deemed appropriate for perturbing rainfalls and temperatures
361 in the present research.

362 Finally, the rain and temperature data can then be spatially distributed over the
363 catchment, using an appropriate kriging procedure, to generate the required input data
364 for the hydrogeological simulations.

365 *2.2.3. Hydrological Model System*

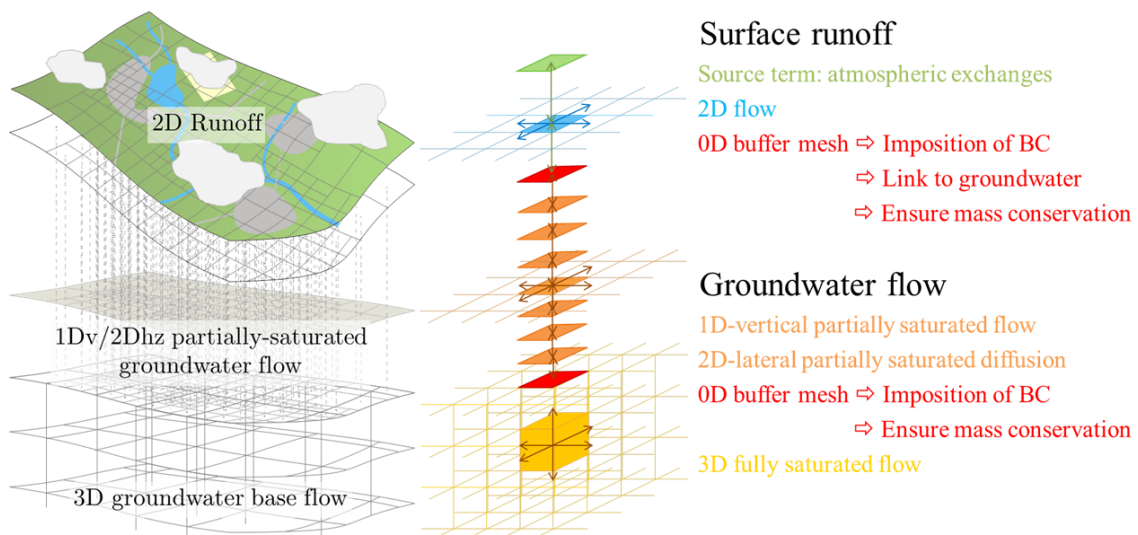
366 A physically based hydrological model is used to simulate water flows at the catchment
367 level. It couples surface and groundwater flow modeling, as depicted in Figure 6
368 (Paulus et al. 2013). The surface runoff model was extensively described by Khuat Duy
369 et al. (2010) and Dewals et al. (2012). The groundwater part of the model involves two
370 layers, which correspond to the saturated and the unsaturated zones. In the former, the
371 flow is computed by solving the three-dimensional (3D) Darcy equations, while the
372 latter is modeled based on an original approach that couples one-dimensional (1D) and
373 two-dimensional (2D) models to approximately solve the Richards equation.

374 Solving the complete 3D Richards equation for the unsaturated zone of real-
375 world catchments is computationally costly (Wildemeersch et al., 2014). Moreover, the
376 focus of the present research is mainly on overland flow, such that an approximate
377 “quasi-3D” resolution of the unsaturated zone was deemed appropriate. It consists of
378 replacing the 3D Richards equation by a set of 1D vertical models plus one 2D
379 horizontal model (see “1Dv/2Dhz partially saturated groundwater flow” in Figure 6).

380 This dramatically reduces the computational cost while reasonably representing the
 381 vertical flow and the horizontal transfers in the unsaturated zone.

382 The models used for overland flow, the unsaturated zone and the saturated zone
 383 are coupled through so-called buffer cells (Figure 6), which accommodate the use of
 384 different time steps and different grid spacings in each model.

385 The main results of these simulations are time series of runoff reaching the
 386 rivers. Using the one-dimensional hydraulic model Wolf1D for flow routing (Khuat
 387 Duy et al. 2010, Dewals et al. 2012), river discharges are calculated at different
 388 locations in the watershed. These discharges are then used for flood-frequency analysis
 389 and serve in the end as input data for the 2D hydraulic model (section 2.2.4.).



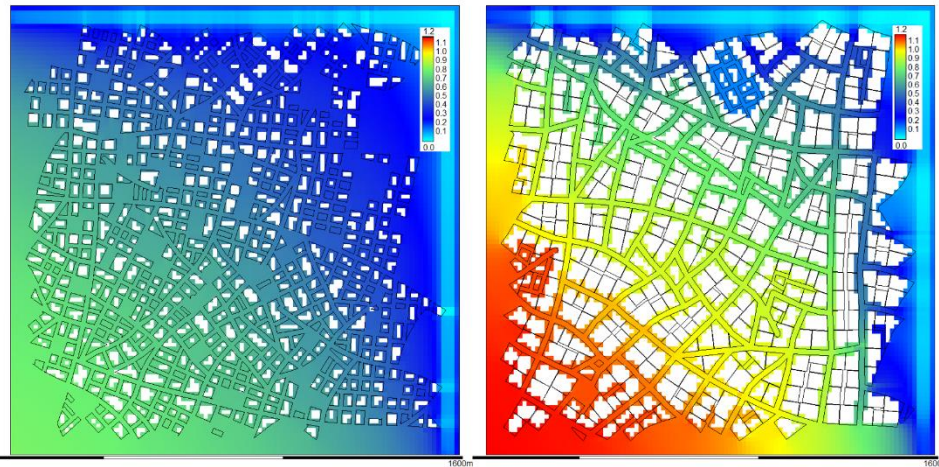
390

391 Figure 6. Coupling between the groundwater model and the surface hydrological model.

392 2.2.4. Hydraulic Model System

393 The hydraulic model aims to simulate the detailed flow characteristics at the level of the
 394 river and its floodplains. It uses the flood discharge and geometric data characterizing
 395 the main riverbed (bathymetry) and the floodplains (topography) as input data. It
 396 delivers detailed information on the inundation extent, the flow depth (Figure 7) and the

397 flow velocity, as outputs, which in turn are used as inputs for exposure assessment and
 398 damage modeling (section 2.2.5).



399
 400 Figure 7: Distribution of water depths computed by the hydraulic model for the same
 401 flood event and two different scenarios of urban development.

402

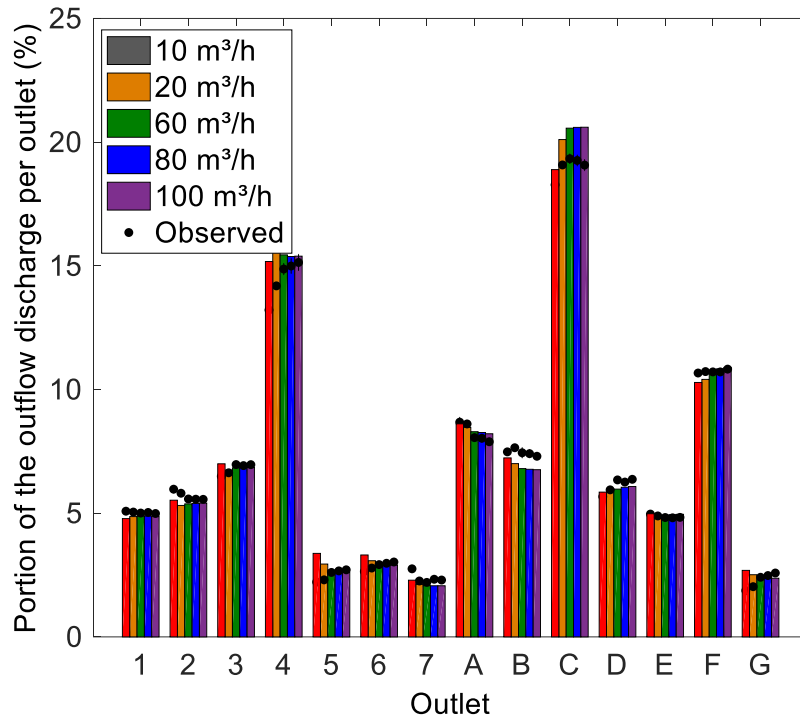
403 High-resolution topographic data obtained from remote sensing techniques are
 404 increasingly available. The typical grid spacing of such data may be as fine as 1 to 5 m.
 405 However, performing detailed flood modeling at such a fine resolution is
 406 computationally demanding, particularly when multiple runs of the hydraulic model are
 407 necessary to assess the influence of uncertainties or various land-use and climate
 408 scenarios. Consequently, the present need is for high-performance computational
 409 models that nonetheless take full benefit of the available detailed topographic data, thus
 410 combining accuracy and high efficiency. One way to meet this challenge is through the
 411 development of subgrid models.

412 Subgrid models enable a decrease of the computational time while preserving
 413 information from the detailed topographic data to some degree. One such sub-grid
 414 modeling approach for simulation of inundation flow consists of solving the shallow-
 415 water equations with porosity. Shallow-water models with porosity are typically applied

416 with a computational cell size of one to two orders of magnitude higher than the size of
417 the available detailed topographic data. The topography is represented through porosity
418 parameters reflecting the storage capacity inside a control volume and the conveyance
419 across the borders of the control volumes.

420 Various shallow-water models with porosity exist. They differ mainly in how
421 the porosity parameters are defined and evaluated. Some authors use porosity as a
422 continuous mathematical field, in which storage porosity remains undistinguished from
423 exchange (conveyance) porosity. Inversely, other authors use porosity as a discrete cell
424 or border property, which enables storage porosity within a cell to be distinguished from
425 exchange porosity at a border. Recently, some authors have used depth-dependent
426 porosity to take into consideration the potential variation of the porosity values with the
427 water depth. Based on quantitative analyses for theoretical and real-world urban areas,
428 we have shown that models greatly benefit from being based on porosities defined as
429 discrete cell or border properties.

430 The model is solved based on a finite volume scheme. A flux vectors splitting
431 technique is used to compute the fluxes across the borders of each cell (Epicum et al.
432 2010a, 2010b). An optimal discretization of the source term representing gravity is
433 achieved, as detailed by Bruwier et al. (2016). The new discrete equations have been
434 implemented in the existing Wolf 2D model, which has already been extensively
435 applied for flood hazard and flood risk analyses (Ernst et al. 2010, Beckers et al. 2013,
436 Bruwier et al. 2015, Detrembleur et al. 2015). The newly coded model has been verified
437 and validated against 1D and 2D, steady and unsteady idealized test cases, as well as
438 against experimental results (Figure 8).



439

440 Figure 8: Satisfactory agreement between computed and observed distributions of the
 441 flow discharge between the different streets of an urban district. Reference data are
 442 from the scale model presented by Arrault et al. (2016).

443 2.2.5. Economic Impact Assessment Module

444 Flood risk is expected to increase in the future due to climate change and urbanization.
 445 While climate change affects flood hazard, urbanization influences flood exposure and
 446 vulnerability. Flood exposure for a given flood discharge and land-use scenario is
 447 evaluated here by overlaying the corresponding land-use map and the inundation maps
 448 obtained from hydraulic modeling. Next, flood damage estimation is performed in two
 449 steps. First, the relative damage is obtained by combining the flood exposure results
 450 with stage-damage curves developed in the framework of the FLEMO model (Kreibich
 451 et al. 2010). Second, for each land-use category or considered urban class, the relative
 452 damage is multiplied by the corresponding inundation extent and by a specific price,

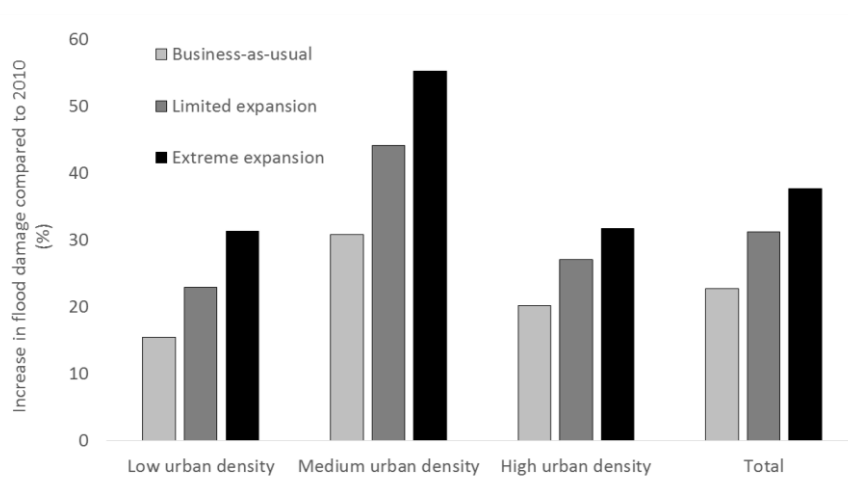
453 leading to the potential damage in absolute terms. This estimation is performed for both
454 mobile and immobile assets.

455 The specific prices are assessed following Beckers et al. (2013), who derived
456 specific prices from ATKIS data (a German database) and adapted them to the case
457 study area. Here, the specific price for each urban class is computed as the product of an
458 average density over all urban cells of a specific urban class and a price per m² of
459 building. This latter price was calibrated such that the flood damage computed here in
460 the baseline scenario corresponds to the baseline damage computed by Beckers et al.
461 (2013).

462 The Land-Use Model System (Section 2.2.1.2) distinguishes between several
463 urban density classes. The influence of the considered number of urban classes on the
464 flood damage estimation was quantified. We found that using more than three different
465 urban classes yields only marginal improvements in the calculations.

466 Figure 9 provides some preliminary results based on the following three urban
467 expansion scenarios for 2030 derived from the coupled cellular automata (CA) and
468 agent-based (AB) urban expansion model: (i) business-as-usual, (ii) limited expansion
469 and (iii) extreme expansion scenarios. The main factor controlling these scenarios is the
470 future demand for urban land. Each urban expansion scenario is developed by including
471 or not including a ban on development in high and/or medium flood hazard zones. The
472 resulting increases in flood damage are between 23 and 38% depending on the urban
473 class (Figure 4). The highest increases in flood damage occur for the medium-density
474 class, while the rise of flood damage for the high-density class is slightly higher than for
475 the low-density class. Additionally, the increase in flooded area is higher for the low-
476 density urban class, but nonetheless, flood damage increases more for the medium-
477 density class where the flood induces higher damage. These results are of particular

478 relevance for risk management as they enable the identification of areas wherein
 479 alternate urbanization policies could be implemented to mitigate future flood risk.



480

481 Figure 9: Increase in flood damage due to future urbanization for the horizon 2030
 482 compared to the baseline situation (2010).

483

484 Regarding the assessment of the indirect economic impact, an Input-Output (I-
 485 O) model is being developed. The advantage of using an I-O approach is that it can
 486 easily be associated with the standard freight model (Section 2.2.1). The freight model
 487 plays the role of intermediate between the physical damage of the transportation
 488 network and the commodity flows subjected to eventual impacts. The Input-Output
 489 model will be calibrated using the I-O tables stemming from the Federal Planning
 490 Bureau using the NACE code referencing system. Preliminary results reported in Saadi
 491 et al. (2016c) show the efficiency of the I-O model in capturing the higher-order
 492 economic impacts.

493

494 2.2.6. Policy Module

495 The policy module steers the different policy and urbanization scenarios in the
496 modeling chain. With respect to future urbanization, the following three groups of
497 scenarios are proposed: (i) business-as-usual scenarios, (ii) an urban intensification
498 scenario and
499 (iii) a sustainable scenario.

500 The business-as-usual scenarios extrapolate the existing urbanization trends.
501 Based on linear extrapolations of the urban expansion and intensification (low, medium
502 and high density) between 1990, 2000 and 2010, the following three scenarios will be
503 generated: low, medium and high demand. These scenarios were derived by
504 respectively extrapolating the trends between 2000 and 2010, 1990 and 2010, and 1990
505 and 2000.

506 The intensification scenario stops developing new urban lands and alternatively
507 intensifies existing ones. This scenario increases the vulnerability of high-density urban
508 areas to flooding when they are located in places at risk.

509 The sustainable scenario suggests stopping the development of new lands and
510 intensifying existing ones, those more exposed to flood risks (lowlands), following the
511 “Room-for-the-River” policy adopted in the Netherlands. The lowlands are meant to
512 receive the peak discharge of the river in flooding cases to prevent flooding in other
513 areas. The low- and medium-density lands outside lowlands are intensified until specific
514 thresholds are met. The definition of these thresholds is based on average density values
515 for settlements that are homogeneous. The remaining required urban areas will be
516 expanded outside existing ones.

517

518

519

520 **3. Further development of the LUTI model**

521 With respect to further developments, a key challenge lies in ensuring the
522 interoperability of the different modules of the integrated modeling framework. If we
523 focus on the land-use transport interaction model, the development of the input-output
524 models is especially essential, as it offers the required methodology to correctly
525 represent the relationship between economic systems and transport systems (Bachmann,
526 Kennedy, and Roorda 2014). To develop the model, the activity locations should be
527 derived from the land-use modeling component. A disaggregation of the freight demand
528 model would serve, in this case, as an excellent starting point for the input-output
529 model.

530 The accessibility measures, which are used in the land-use change models to
531 determine the transition probabilities, should ideally reflect the generalized cost
532 structure of the transportation network. To this end, the integration of (dynamic) traffic
533 assignment of passenger and freight traffic will better reflect the actual load profiles on
534 the network and correspondingly provide more realistic accessibility measures.

535 A final enhancement of the LUTI model concerns the feedback toward the
536 climatological forecasts and inclusion of the reverse direct effect. After all,
537 meteorological conditions also affect activity-travel patterns (Creemers, Cools, and
538 Wets 2015).

539 **4. Conclusions**

540 In this research paper, we have discussed the development trajectory of an integrated
541 framework for assessing spatial planning scenarios that could alleviate the negative
542 effects associated with future river floods. To this end, we have considered a complete
543 risk chain, from climate impact, via hydrological and hydraulic modeling, to damage
544 and risk estimation using land-use transport interaction models.

545

546 The presentation of the design of the framework and discussion of the
547 developments of the different submodules has highlighted the added value and potential
548 of using LUTI models in the context of the development of a methodology for risk
549 assessment.

550 One of the most significant challenges of this research lies in the coupling of
551 different modeling tools, spanning from socio-economic to physical/hydrological
552 aspects. In addition to interoperability issues, this research will require addressing the
553 chain of uncertainties inherent in such approaches, especially when one considers a
554 2100 horizon.

555 Future research will focus on the development of different scenarios combining
556 climatological and land-use change scenarios to quantify the influence of micro-scale
557 spatial patterns in future land-use on flood hazard, exposure and risk. The developed
558 models and methodology will be validated and demonstrated on a real-world case study
559 corresponding to a Belgian sub-basin (Ourthe river) of the international Meuse basin.

560 **5. Acknowledgments**

561 The research was funded through the ARC grant for Concerted Research Actions and
562 through the Special Fund for research, both financed by the Wallonia-Brussels
563 Federation.

564 **6. References**

565 Aljoufie M., M. Zuidgeest, M. Brussel, J. van Vliet, and M. van Maarseveen. 2013. “A
566 cellular automata-based land use and transport interaction model applied to Jeddah,
567 Saudi Arabia.” *Landscape and Urban Planning* 112: 89–99.
568 doi:10.1016/j.landurbplan.2013.01.003.

- 569 Arrault, A., P. Finaud-Guyot, P. Archambeau, M. Bruwier, S. Erpicum, M. Piroton,
570 and B. Dewals. 2016. “Hydrodynamics of long-duration urban floods: Experiments
571 and numerical modelling.” *Natural Hazards and Earth System Sciences* 16 (6): 1413–
572 1429. doi:10.5194/nhess-16-1413-2016.
- 573 Augustijn-Beckers E. W., J. Flacke, and B. Retsios. 2011. “Simulating informal
574 settlement growth in Dar es Salaam, Tanzania: An agent-based housing model.”
575 *Computers, Environment and Urban Systems* 35 (2): 93–103.
576 doi:10.1016/j.compenvurbsys.2011.01.001.
- 577 Auld J., and A. Mohammadian. 2009. “Framework for the development of the agent-
578 based dynamic activity planning and travel scheduling (adapts) model.”
579 *Transportation Letters: The International Journal of Transportation Research* 1 (3):
580 245–255. doi:10.3328/TL.2009.01.03.245-255.
- 581 Bachmann C., C. Kennedy, M. J. Roorda. 2014. “Applications of Random-Utility-based
582 Multi-region Input–Output Models of Transport and the Spatial Economy.” *Transport*
583 *Reviews* 34 (4): 418–440. doi:10.1080/01441647.2014.907369.
- 584 Balmer M., K. Axhausen, and K. Nagel. 2006. “Agent-Based Demand-Modeling
585 Framework for Large-Scale Microsimulations.” *Transportation Research Record:*
586 *Journal of the Transportation Research Board* 1985: 125–134. doi:10.3141/1985-14.
- 587 Batty M., Y. Xie, and Z. Sun. 1999. “Modeling urban dynamics through GIS-based
588 cellular automata.” *Computers, Environment and Urban Systems* 23 (3): 205–233.
589 doi:10.1016/S0198-9715(99)00015-0.
- 590 Beckers A., B. Dewals, S. Erpicum, S. Dujardin, S. Detrembleur, J. Teller, M. Piroton,
591 and P. Archambeau. 2013. “Contribution of land use changes to future flood damage
592 along the river Meuse in the Walloon region.” *Natural Hazards and Earth System*
593 *Sciences* 13 (9): 2301–2318. doi:10.5194/nhess-13-2301-2013.

- 594 Beckman R. J., K. A. Baggerly, and M. D. McKay. 1996. "Creating synthetic baseline
595 populations." *Transportation Research Part A: Policy and Practice* 30 (6): 415–429.
596 doi:10.1016/0965-8564(96)00004-3.
- 597 Bert F. E., G. P. Podestá, S. L. Rovere, A. N. Menéndez, M. North, E. Tatara, C. E.
598 Laciana, E. Weber, F. R. Toranzo. 2011. "An agent based model to simulate structural
599 and land use changes in agricultural systems of the argentine pampas." *Ecological*
600 *Modelling* 222 (19): 3486–3499. doi:10.1016/j.ecolmodel.2011.08.007.
- 601 Bruwier, M., S. Erpicum, M. Piroton, P. Archambeau, and B. J. Dewals. 2015.
602 "Assessing the operation rules of a reservoir system based on a detailed modelling
603 chain." *Natural Hazards and Earth System Sciences* 15 (3): 365–379.
604 doi:10.5194/nhess-15-365-2015.
- 605 Bruwier, M., P. Archambeau, S. Erpicum, M. Piroton, and B. Dewals. 2016.
606 "Discretization of the divergence formulation of the bed slope term in the shallow-
607 water equations and consequences in terms of energy balance." *Applied Mathematical*
608 *Modelling* 40 (17-18): 7532-7544. doi: 10.1016/j.apm.2016.01.041.
- 609 Cornelis E., M. Hubert, P. Hunyen, K. Lebrun, G. Patriarche, A. De Witte, L. Creemers,
610 et al. 2012. *Belgian Daily Mobility (BELDAM): Enquête sur la mobilité quotidienne*
611 *des belges*. Brussels: SPF Mobilité & Transports.
- 612 Creemers L., G. Wets, and M. Cools. 2015. "Meteorological variation in daily travel
613 behaviour: evidence from revealed preference data from the Netherlands." *Theoretical*
614 *and Applied Climatology* 120 (1): 183–194. doi:10.1007/s00704-014-1169-0.
- 615 Detrembleur, S., F. Stilmant, B. Dewals, S. Erpicum, P. Archambeau, M. Piroton.
616 2015. "Impacts of climate change on future flood damage on the river Meuse, with a
617 distributed uncertainty analysis." *Natural Hazards* 77 (3): 1533–1549.
618 doi:10.1007/s11069-015-1661-6.

- 619 Devillet G., M. Jaspard, J. Vazquez Parras. 2014. *Atlas du commerce en Wallonie.*
620 *Structures, Dynamiques, Comportements spatiaux des consommateurs.* Liège, Presses
621 universitaires de Liège.
- 622 Dewals, B. J., P. Archambeau, P., B. Khuat Duy, S. Erpicum, and M. Pirotton. 2012.
623 “Semi-explicit modelling of watersheds with urban drainage systems.” *Engineering*
624 *Applications of Computational Fluid Mechanics*, 6(1), 46–57.
- 625 Drogue G., L. Pfister, T. Leviandier, A. El Idrissi, J. F. Iffly, P. Matgen, J. Humbert,
626 and L. Hoffmann. 2004. “Simulating the spatio-temporal variability of streamflow
627 response to climate change scenarios in a mesoscale basin.” *Journal of Hydrology* 293
628 (1–4): 255–269. doi:10.1016/j.jhydrol.2004.02.009.
- 629 Du Y., W. Wen, F. Cao, and M. Ji. 2010. “A case-based reasoning approach for land
630 use change prediction.” *Expert Systems with Applications* 37 (8): 5745–5750.
631 doi:10.1016/j.eswa.2010.02.035.
- 632 Elmer F., J. Hoymann, D. DÜthmann, S. Vorogushyn, H. Kreibich. 2012. “Drivers of
633 flood risk change in residential areas.” *Natural Hazards and Earth System Sciences* 12
634 (5): 1641–1657. doi:10.5194/nhess-12-1641-2012.
- 635 Erpicum S., B. Dewals, P. Archambeau, S. Detrembleur, and M. Pirotton. 2010a.
636 “Detailed Inundation Modelling Using High Resolution DEMs.” *Engineering*
637 *Applications of Computational Fluid Mechanics* 4 (2): 196–208.
638 doi:10.1080/19942060.2010.11015310.
- 639 Erpicum S., B. Dewals, P. Archambeau, and M. Pirotton. 2010b. “Dam break flow
640 computation based on an efficient flux vector splitting.” *Journal of Computational and*
641 *Applied Mathematics* 234 (7): 2143–2151. doi:10.1016/j.cam.2009.08.110.
- 642 Ernst, J., B. J. Dewals, S. Detrembleur, P. Archambeau, S. Erpicum, and M. Pirotton.
643 2010. “Micro-scale flood risk analysis based on detailed 2D hydraulic modelling and

- 644 high resolution geographic data". *Natural Hazards* 55(2), 181–209.
645 doi:10.1007/s11069-010-9520-y.
- 646 Farooq B., M. Bierlaire, R. Hurtubia, and G. Flötteröd. 2013. "Simulation based
647 population synthesis." *Transportation Research Part B: Methodological* 58: 243–63.
648 doi:10.1016/j.trb.2013.09.012.
- 649 García A. M., I. Santé, R. Crecente, and D. Miranda. 2011. "An analysis of the effect of
650 the stochastic component of urban cellular automata models." *Computers,*
651 *Environment and Urban Systems* 35 (4): 289–296.
652 doi:10.1016/j.compenvurbsys.2010.11.001.
- 653 Goderniaux P., S. Brouyère, S. Blenkinsop, A. Burton, H. J. Fowler, P. Orban, and A.
654 Dassargues. 2011. "Modeling climate change impacts on groundwater resources using
655 transient stochastic climatic scenarios." *Water Resources Research* 47 (12).
656 doi:10.1029/2010WR010082.
- 657 Goderniaux P., S. Brouyère, S. Wildemeersch, R. Therrien, and A. Dassargues. 2015.
658 "Uncertainty of climate change impact on groundwater reserves – Application to a
659 chalk aquifer." *Journal of Hydrology* 528: 108–121.
660 doi:10.1016/j.jhydrol.2015.06.018.
- 661 Guan D., H. Li, T. Inohae, W. Su, T. Nagaie, and K. Hokao. 2011. "Modeling urban
662 land use change by the integration of cellular automaton and Markov model."
663 *Ecological Modelling* 222 (20–22): 3761–3772. doi:10.1016/j.ecolmodel.2011.09.009.
- 664 Guo J. Y., and C. R. Bhat. 2007. "Population Synthesis for Microsimulating Travel
665 Behavior." *Transportation Research Record: Journal of the Transportation Research*
666 *Board* 2014: 92–101. doi:10.3141/2014-12.

- 667 He Y., J. Zhou, P. Kou, N. Lu, and Q. Zou. 2011. "A fuzzy clustering iterative model
668 using chaotic differential evolution algorithm for evaluating flood disaster." *Expert*
669 *Systems with Applications* 38 (8): 10060–10065. doi:10.1016/j.eswa.2011.02.003.
- 670 Henson K., K. Goulias, and R. Golledge. 2009. "An assessment of activity-based
671 modeling and simulation for applications in operational studies, disaster preparedness,
672 and homeland security." *Transportation Letters: The International Journal of*
673 *Transportation Research* 1(1): 19–39. doi:10.3328/TL.2009.01.01.19-39.
- 674 Holguín-Veras J., M. Jaller, I. Sánchez-Díaz, S. Campbell, and C. T. Lawson. 2014. "3 -
675 Freight Generation and Freight Trip Generation Models." In *Modelling Freight*
676 *Transport*, edited by L. Tavasszy, and G. de Jong, 43-63. Oxford: Elsevier.
677 doi:10.1016/B978-0-12-410400-6.00003-3.
- 678 Hosseinali F., A. A. Alesheikh, and F. Nourian. 2013. "Agent-based modeling of urban
679 land-use development, case study: Simulating future scenarios of Qazvin city." *Cities*
680 31: 105–113. doi:10.1016/j.cities.2012.09.002.
- 681 Jenelius E., and L. G. Mattsson. 2015. "Road network vulnerability analysis:
682 Conceptualization, implementation and application." *Computers, Environment and*
683 *Urban Systems* 49: 136–147. doi:10.1016/j.compenvurbsys.2014.02.003.
- 684 Jonkman S.N., M. Bockarjova, M. Kok, and P. Bernardini. 2008. "Integrated
685 hydrodynamic and economic modelling of flood damage in the Netherlands." *Ecological Economics* 66 (1): 77–90. doi:10.1016/j.ecolecon.2007.12.022.
- 687 Jun K. S., E. S. Chung, Y. G. Kim, Y. Kim. 2013. "A fuzzy multi-criteria approach to
688 flood risk vulnerability in south korea by considering climate change impacts." *Expert*
689 *Systems with Applications* 40 (4): 1003–1013. doi:10.1016/j.eswa.2012.08.013.
- 690 Khuat Duy, B., P. Archambeau, B. J. Dewals, S. Erpicum, and M. Pirotton. 2010.
691 "River modeling and flood mitigation in a Belgian catchment." *Proceedings of the*

- 692 *Institution of Civil Engineers: Water Management*, 163 (8): 417–423. doi:
693 10.1680/wama.900042.
- 694 Kreibich, H., I. Seifert, B. Merz, and A. H. Thielen. 2010. “Development of FLEMOcs
695 – a new model for the estimation of flood losses in the commercial sector”
696 *Hydrological Sciences Journal* 55 (8): 1302-1314.
697 doi:10.1080/02626667.2010.529815
- 698 Kundzewicz Z., U. Ulbrich, T. Brücher, D. Graczyk, A. Krüger, G. Leckebusch, L.
699 Menzel, I. Piskwar, M. Radziejewski, M. Szwed. 2005. “Summer floods in central
700 Europe – climate change track?” *Natural Hazards* 36 (1): 165–189.
701 doi:10.1007/s11069-004-4547-6.
- 702 Lawson C., J. Holguín-Veras, I. Sánchez-Díaz, M. Jaller, S. Campbell, and E. Powers.
703 2012. “Estimated Generation of Freight Trips Based on Land Use.” *Transportation*
704 *Research Record: Journal of the Transportation Research Board* 2269: 65–72.
705 doi:10.3141/2269-08.
- 706 Liu F., D. Janssens, J. Cui, G. Wets, and M. Cools. 2015. “Characterizing activity
707 sequences using profile Hidden Markov Models.” *Expert Systems with Applications* 42
708 (13): 5705–5722. doi:10.1016/j.eswa.2015.02.057.
- 709 Mitsova D., W. Shuster, and X. Wang. 2011. “A cellular automata model of land cover
710 change to integrate urban growth with open space conservation.” *Landscape and*
711 *Urban Planning* 99 (2): 141–153. doi:10.1016/j.landurbplan.2010.10.001.
- 712 Munich RE. 2010. *Topics GEO - Natural catastrophes 2009: Analyses, assessments,*
713 *positions*. Munich: Munich RE.
- 714 Mustafa A. M., M. Cools, I. Saadi, and J. Teller. 2015a. “Urban Development as a
715 Continuum: A Multinomial Logistic Regression Approach”. In *Computational Science*
716 *and Its Applications – ICCSA 2015*, edited by O. Gervasi, B. Murgante, S. Misra, M.

- 717 L. Gavrilova, A. M. A. C. Rocha, C. Torre, D. Taniar, and B. O., 729-744. Cham:
718 Springer. doi:10.1007/978-3-319-21470-2_53.
- 719 Mustafa A., I. Saadi, M. Cools, and J. Teller. 2014. "Measuring the Effect of Stochastic
720 Perturbation Component in Cellular Automata Urban Growth Model." *Procedia
721 Environmental Sciences* 22: 156–168. doi:10.1016/j.proenv.2014.11.016.
- 722 Mustafa A., I. Saadi, M. Cools, and J. Teller. 2015b. "Modelling Uncertainties in Long-
723 Term Predictions of Urban Growth: A Coupled Cellular Automata and Agent-Based
724 Approach." In *Proceedings of the 14th International Conference on Computers in
725 Urban Planning and Urban Management*. Cambridge, MA: Massachusetts Institute of
726 Technology.
- 727 Ntegeka V., P. Baguis, E. Roulin, and P. Willems. 2014. "Developing tailored climate
728 change scenarios for hydrological impact assessments." *Journal of Hydrology* 508:
729 307–321. doi:10.1016/j.jhydrol.2013.11.001.
- 730 Paulus, R., Dewals, B. J., Erpicum, S., Piroton, M., & Archambeau, P. (2013).
731 "Innovative modelling of 3D unsaturated flow in porous media by coupling
732 independent models for vertical and lateral flows." *Journal of Computational and
733 Applied Mathematics*, 246, 38–51. doi: 10.1016/j.cam.2012.07.032.
- 734 Pendyala R., C. Bhat, K. Goulias, R. Paleti, K. Konduri, R. Sidharthan, H. H. Hu, G.
735 Huang, K. Christian. 2012. "Application of Socioeconomic Model System for
736 Activity-Based Modeling." *Transportation Research Record: Journal of the
737 Transportation Research Board* 2303: 71–80. doi:10.3141/2303-08.
- 738 Poelmans L., A. Van Rompaey, and O. Batelaan. 2010. "Coupling urban expansion
739 models and hydrological models: How important are spatial patterns?" *Land Use
740 Policy* 27 (3):965–975. doi:10.1016/j.landusepol.2009.12.010.

- 741 Pontius Jr R. G., D. Huffaker, K. Denman. 2004. "Useful techniques of validation for
742 spatially explicit land-change models." *Ecological Modelling* 179 (4) :445–461.
743 doi:10.1016/j.ecolmodel.2004.05.010.
- 744 Pritchard D. R., and E. J. Miller. 2012. "Advances in population synthesis: fitting many
745 attributes per agent and fitting to household and person margins simultaneously." *Transportation* 39 (3): 685–704. doi:10.1007/s11116-011-9367-4.
- 747 Ralha C. G., C. G. Abreu, C. G. C. Coelho, A. Zaghetto, B. Macchiavello, and R. B.
748 Machado. 2013. "A multi-agent model system for land-use change simulation." *Environmental Modelling & Software* 42: 30–46. doi:10.1016/j.envsoft.2012.12.003.
- 749
- 750 Rasouli S., and H. Timmermans. 2014. "Activity-based models of travel demand:
751 promises, progress and prospects." *International Journal of Urban Sciences* 18 (1):
752 31–60. doi:10.1080/12265934.2013.835118.
- 753 Saadi, I., F. Liu,, A. Mustafa, J. Teller, and M. Cools. 2016a. "A framework to identify
754 housing location patterns using profile Hidden Markov Models." *Advanced Science*
755 *Letters* 22 (9): 2117–2121.
- 756 Saadi, I., A. Mustafa, J. Teller, and M. Cools. 2016b. "Forecasting Travel Behavior
757 Using Markov Chains-Based Approaches." *Transportation Research Part C:*
758 *Emerging Technologies* 69: 402–417. doi:10.1016/j.trc.2016.06.020.
- 759 Saadi, I., A. Mustafa, J. Teller, and M. Cools. 2016c. "Évaluation des impacts
760 économiques indirects selon un scénario de risque d'inondation". In *Recueil des*
761 *articles des 34èmes Rencontres Universitaires de Génie Civil de l'AUGC*. Liège:
762 Université de Liège.
- 763 Saadi, I., A. Mustafa, J. Teller, B. Farooq, and M. Cools. 2016d. "Hidden Markov
764 Model-Based Population Synthesis." *Transportation Research Part B:*
765 *Methodological* 90: 1–21. doi:10.1016/j.trb.2016.04.007.

- 766 Saadi, I., J. Teller, and M. Cools. 2016. "Belgium: The Use of MATSim within an
767 Estimation Framework for Assessing Economic Impacts of River Floods." In *The*
768 *Multi-Agent Transport Simulation MATSim*, edited by A. Horni, K. Nagel, and K. W.
769 Axhausen, 399–404. London, UK: Ubiquity Press.
- 770 Sohn J. 2006. "Evaluating the significance of highway network links under the flood
771 damage: An accessibility approach." *Transportation Research Part A: Policy and*
772 *Practice* 40 (6): 491–506. doi:10.1016/j.tra.2005.08.006.
- 773 Suarez P., W. Anderson, V. Mahal, T. R. Lakshmanan. 2005. "Impacts of flooding and
774 climate change on urban transportation: A systemwide performance assessment of the
775 Boston Metro Area." *Transportation Research Part D: Transport and Environment* 10
776 (3): 231–244. doi:10.1016/j.trd.2005.04.007.
- 777 Thieken A. H., H. Cammerer, C. Dobler, J. Lammel, and F. Schöberl. 2014. "Estimating
778 changes in flood risks and benefits of non-structural adaptation strategies - a case
779 study from Tyrol, Austria." *Mitigation and Adaptation Strategies for Global Change*
780 21 (3): 343–376. doi:10.1007/s11027-014-9602-3.
- 781 van Pelt S. C., J. J. Beersma, T. A. Buishand, B. J. J. M. van den Hurk, and P. Kabat.
782 2012. "Future changes in extreme precipitation in the Rhine basin based on global
783 and regional climate model simulations." *Hydrology and Earth System Sciences* 16
784 (12): 4517–4530. doi:10.5194/hess-16-4517-2012.
- 785 van Pelt S. C., P. Kabat, H. W. ter Maat, B. J. J. M. van den Hurk, and A. H. Weerts.
786 2009. "Discharge simulations performed with a hydrological model using bias
787 corrected regional climate model input." *Hydrology and Earth System Sciences* 13
788 (12): 2387–2397. doi:10.5194/hess-13-2387-2009.
- 789 Vansteenkiste T., M. Tavakoli, V. Ntegeka, P. Willems, F. De Smedt, O. Batelaan.
790 2013. "Climate change impact on river flows and catchment hydrology: a comparison

791 of two spatially distributed models.” *Hydrological Processes* 27 (25): 3649–3662.
792 doi:10.1002/hyp.9480.

793 Wang H., S. He, X. Liu, L. Dai, P. Pan, S. Hong, and W. Zhang. 2013. “Simulating
794 urban expansion using a cloud-based cellular automata model: A case study of
795 Jiangxia, Wuhan, China.” *Landscape and Urban Planning* 110: 99–112.
796 doi:10.1016/j.landurbplan.2012.10.016.

797 Wildemeersch, S., P. Goderniaux, P. Orban, S. Brouyère, and A. Dassargues. 2014.
798 “Assessing the effects of spatial discretization on large-scale flow model performance
799 and prediction uncertainty.” *Journal of Hydrology* 510: 10–25.
800 doi:10.1016/j.jhydrol.2013.12.020.

801 Ye X., K. C. Konduri, R. M. Pendyala, B. Sana, and P. Waddell. 2009. “Methodology
802 to Match Distributions of Both Household and Person Attributes in Generation of
803 Synthetic Populations.” In *Proceedings of 88th Annual Meeting of the Transportation
804 Research Board*. Washington, DC: Transportation Research Board of the National
805 Academies.

806